Pre-steady-State Currents in Neutral Amino Acid Transporters Induced by Photolysis of a New Caged Alanine Derivative†

Zhou Zhang,‡ George Papageorgiou,§ John E. T. Corrie,§ and Christof Grewer*,‡

Department of Physiology and Biophysics, University of Miami School of Medicine, 1600 Northwest 10th Avenue, Miami, Florida 33136, and MRC National Institute for Medical Research, The Ridgeway, Mill Hill, London NW7 1AA, United Kingdom

Received October 6, 2006; Revised Manuscript Received December 20, 2006

ABSTRACT: Na^+-Dependent transmembrane transport of small neutral amino acids, such as glutamine and alanine, is mediated, among others, by the neutral amino acid transporters of the solute carrier 1 [SLC1, alanine serine cysteine transporter 1 (ASCT1), and ASCT2] and SLC38 families [sodium-coupled neutral amino acid transporter 1 (SNAT1), SNAT2, and SNAT4]. Many mechanistic aspects of amino acid transport by these systems are not well-understood. Here, we describe a new photolabile alanine derivative based on protection of alanine with the 4-methoxy-7-nitroindolinyl (MNI) caging group, which we use for pre-steady-state kinetic analysis of alanine transport by ASCT2, SNAT1, and SNAT2. MNI-alanine has favorable photochemical properties and is stable in aqueous solution. It is also inert with respect to the transport systems studied. Photolytic release of free alanine results in the generation of significant transient current components in HEK293 cells expressing the ASCT2, SNAT1, and SNAT2 proteins. In ASCT2, these currents show biphasic decay with time constants, τ, in the 1−30 ms time range. They are fully inhibited in the absence of extracellular Na^+, demonstrating that Na^+ binding to the transporter is necessary for induction of the alanine-mediated current. For SNAT1, these transient currents differ in their time course ($\tau = 1.6$ ms) from previously described pre-steady-state currents generated by applying steps in the membrane potential ($\tau \sim 4-5$ ms), indicating that they are associated with a fast, previously undetected, electrogenic partial reaction in the SNAT1 transport cycle. The implications of these results for the mechanisms of transmembrane transport of alanine are discussed. The new caged alanine derivative will provide a useful tool for future, more detailed studies of neutral amino acid transport.

Neutral amino acids are transported across cell membranes by a variety of transport systems (reviewed in ref *1*). Some of these systems, which actively transport neutral amino acids against a concentration gradient, are powered by the co-transport of Na^+ down its own transmembrane concentration gradient. For small neutral amino acids, these systems include system N, system A, and system ASC. System N and system A belong to the same solute carrier (SLC)[1] protein family (SLC38), and the known cloned members of this family have collectively been termed sodium-coupled neutral amino acid transporters (SNATs) (*2*). Members 1, 2, and 4 of this family are thought to belong to the system A class (*3*, *4*), whereas members 3 and 5 belong to the system N class (*5*, *6*). In contrast, system ASC transporters belong to the SLC1 family of transport proteins, and the cloned members alanine serine cysteine transporter 1 (ASCT1) and ASCT2 have a high degree of sequence similarity with glutamate transporters (*7*−*9*).

Pre-steady-state kinetic techniques have been used in the past to study details of the transport mechanism of ion pumps (*10*, *11*) and secondary transporters (*12*−*14*). One way to obtain pre-steady-state kinetic data is to disturb an existing transporter steady state by the application of step changes in the membrane potential and to monitor the relaxation to a new steady state (*15*). This technique has been widely applied to many types of secondary transporters, including SNAT1 (*16*). A second method is based on applying concentration jumps of the transported substrate to the carrier while keeping the membrane potential constant, which also leads to relaxation to a new steady state. This method has been used with glutamate (*12*, *17*) and γ-aminobutyric acid (GABA) transporters (*18*) and has yielded a wealth of new information regarding the transport mechanism. However, rapid reactions of these secondary transporters were found to take place on the sub-millisecond to millisecond time scale (*14*), which makes substrate concentration jumps difficult to achieve with rapid mixing techniques. The technique of flash photolysis of a photolabile ("caged") precursor can produce faster concentration jumps, with the release of

†This work was supported by grants from the Florida Department of Health (04NIR-07) and the National Institutes of Health (R01-NS049335-02) awarded to C.G.

* To whom correspondence should be addressed. Telephone: (305) 243-1021. Fax: (305) 243-5931. E-mail: cgrewer@med.miami.edu.

‡ University of Miami.

§ MRC National Institute for Medical Research.

[1] Abbreviations: ASCT, alanine serine cysteine transporter; Boc, *tert*-butoxycarbonyl; BzlSer, benzylserine; DMAP, 4-dimethylaminopyridine; EGTA, ethylene glycol-bis(2-aminoethylether)-*N*,*N*,*N*′,*N*′-tetraacetic acid; GABA, γ-aminobutyric acid; HEK, human embryonic kidney; HEPES, 4-(2-hydroxyethyl)piperazine-1-ethanesulfonic acid; MNI, 4-methoxy-7-nitroindolinyl; NMG^+, *N*-methylglucamine$^+$; SLC, solute carrier; SNAT, sodium-coupled neutral amino acid transporter; TFA, trifluoroacetic acid.

10.1021/bi0620860 CCC: $37.00
Published on Web 02/21/2007

substrates in less than 100 μs being achievable in some cases (*19*). Obviously, this requires the availability of a suitable reagent, and hitherto, there have been no reports of the synthesis and development of caged neutral amino acids as potential caged substrates for SNATs and ASCTs.

Here, we report the synthesis and characterization of a new caged alanine derivative [4-methoxy-7-nitroindolinyl (MNI)-alanine, **4**] that is based on protection with the 4-methoxy-7-nitroindolinyl caging group. The MNI and related nitroindoline caging groups have been used previously to generate caged derivatives of glutamate and glycine (*20*, *21*), and the mechanism and kinetics of product release from these caging groups have been studied. The rate constant for amino acid release is 5×10^6 s^{-1} (*22*). We tested MNI-alanine with three neutral amino acid transporters, namely, ASCT2, SNAT1, and SNAT2, and found that the compound is biologically inactive with respect to these transport systems. Photolysis of MNI-alanine results in the release of free alanine, which activates specific currents in cells expressing ASCT2, SNAT1, or SNAT2. These currents have significant pre-steady-state components, which have not been observed in the past, by using slower transport assays.

MATERIALS AND METHODS

*Synthesis of MNI-Alanine: 1-[2S-2-(tert-Butoxycarbonylamino)propanoyl]-4-methoxyindoline (**1**).* A solution of crude 4-methoxyindoline (1.04 g, 7 mmol), prepared as previously described (*23*), in dry MeCN (40 mL) was treated with *N-tert*-butoxycarbonyl (Boc)-alanine (1.46 g, 7.7 mmol) and 1-(3-dimethylaminopropyl)-3-ethylcarbodiimide·HCl (1.88 g, 9.8 mmol) and stirred at room temperature for 18 h. The solvent was evaporated, and the residue was dissolved in EtOAc (80 mL), washed with 0.5 M aqueous HCl, saturated aqueous $NaHCO_3$, and brine, dried, and evaporated to give **1** as white crystals (1.57 g, 70%), with mp = 156−158 °C (EtOAc/hexanes). ^{1}H NMR (500 MHz, $CDCl_3$) δ: 7.83 (1H, d, J = 8.1 Hz, H-7), 7.18 (1H, t, J = 8.1 Hz, H-6), 6.61 (1H, d, J = 8.1 Hz, H-5), 5.45 (1H, d, J = 7.8 Hz, NH), 4.54−4.56 (1H, m, CH), 4.26−4.34 (1H, m, H-2), 4.06−4.12 (1H, m, H-2), 3.84 (3H, s, OMe), 3.10−3.16 (2H, m, H-3), 1.44 (9H, s, CMe_3), 1.39 (3H, d, J = 6.9 Hz, Me). Anal. Calcd for $C_{17}H_{24}N_2O_4$: C, 63.73; H, 7.55; N, 8.74. Found: C, 63.56; H, 7.72; N, 8.69.

*1-[2S-2-(Di-tert-butoxycarbonylamino)propanoyl]-4-methoxyindoline (**2**).* A solution of **1** (0.96 g, 3 mmol) in a mixture of dry CH_2Cl_2 (12 mL) and Et_3N (18 mL) was treated with di-*tert*-butyl dicarbonate (1.64 g, 7.5 mmol) and 4-dimethylaminopyridine (DMAP, 37 mg, 0.3 mmol) and refluxed under nitrogen for 6 h. The solvents were evaporated, and the residue was diluted with EtOAc (50 mL), washed with 1 M $KHSO_4$, saturated aqueous $NaHCO_3$, and brine, dried, and evaporated. Flash chromatography [EtOAc/hexanes (1:4)] followed by trituration with Et_2O/hexanes gave **2** as white crystals (1.04 g, 82%), with mp = 56−58 °C (hexanes). ^{1}H NMR (500 MHz, $CDCl_3$) δ: 7.79 (1H, d, J = 8.1 Hz, H-7), 7.16 (1H, t, J = 8.1 Hz, H-6), 6.60 (1H, d, J = 8.1 Hz, H-5), 5.01 (1H, q, J = 6.5 Hz, CH), 4.01 (2H, t, J = 8.3 Hz, H-2), 3.83 (3H, s, OMe), 3.06 (2H, t, J = 8.3 Hz, H-3), 1.52 (3H, d, J = 6.7 Hz, Me), 1.48 (18H, s, 2× CMe_3). Anal. Calcd for $C_{22}H_{32}N_2O_6 \cdot {}^1/_2H_2O$: C, 61.52; H, 7.75; N, 6.52. Found: C, 61.69; H, 7.71; N, 6.48.

*1-[2S-2-Aminopropanoyl]-4-methoxy-7-nitroindoline (**4**).* Claycop [1.28 g, prepared as previously described (*28*)] was added to a solution of **2** (0.84 g, 2 mmol) in a mixture of acetic anhydride (6 mL) and CCl_4 (12 mL), and the mixture was stirred at room temperature for 6 h. The solid was filtered off and washed thoroughly with EtOAc, and the filtrate was evaporated. The residue was taken up with EtOAc (50 mL), washed with saturated aqueous $NaHCO_3$ and brine, dried, and evaporated to a brown, viscous oil (765 mg). This was dissolved in CH_2Cl_2 (20 mL), treated with dilute trifluoroacetic acid (TFA; 1 M solution in CH_2Cl_2; 3 mL, 3 mmol), and stirred at room temperature for 20 h. The solvent was evaporated, and the residue was dissolved in EtOAc (40 mL), washed with saturated aqueous $NaHCO_3$ and brine, dried, and evaporated. Flash chromatography [EtOAc/hexanes (3:7)] gave 1-[2*S*-2-(*tert*-butoxycarbonylamino)propanoyl]-4-methoxy-7-nitroindoline (**3**) as a yellow viscous oil (0.47 g), slightly contaminated with the 5-nitro isomer. This material (327 mg, 0.89 mmol) was dissolved in neat TFA (10 mL), stirred at room temperature for 1 h, and concentrated *in vacuo*. The residue was dissolved in water (89 mL), adjusted to pH 7.0 with 1 M aqueous NaOH, washed with ether, and analyzed by reverse-phase high-performance liquid chromatography (HPLC) [mobile phase of 25 mM Na phosphate at pH 6.0/MeOH (10:7, v/v) at 1.5 mL/min], with t_R = 7.2 min. A small peak with t_R = 9.2 min appeared to be the 5-nitro isomer but was not characterized further. The solution was lyophilized, dissolved in 25 mM Na phosphate at pH 6.0 (120 mL), and pumped at 2 mL/min onto a preparative HPLC column (2 × 30 cm, filled with Waters C_{18} packing, catalog number 20594) that was equilibrated in the same phosphate buffer. The column was first eluted with 10 mM Na phosphate at pH 6.0 for 1 h and then with water for 2 h, and the product was eluted with 10 mM Na phosphate at pH 6.0/MeOH (10:4, v/v) (all flow rates = 2 mL/min). Fractions were analyzed as above, and those containing only the main peak (i.e., with t_R = 7.2 min) were combined and concentrated *in vacuo*. The residue was dissolved in water (42 mL) and quantified by UV spectroscopy (using ϵ_{327} = 4800 M^{-1} cm^{-1}; 464 μmol). The aqueous solution was carefully basified to pH 10.5 with 1 M aqueous NaOH and extracted with $CHCl_3$ (3 × 50 mL). The combined organic phases were dried and evaporated, and the residue was dissolved in EtOH (4 mL) and diluted with water (38 mL). The pH was carefully lowered to 6.9 with 1 M aqueous HCl, and the solution was quantified by UV spectroscopy (433 μmol). The solution was lyophilized, and the residual powder was dissolved in water (20 mL), passed through a 0.2 μm membrane filter, and lyophilized again. Finally, the solid was dissolved in water (14 mL) and quantified by UV spectroscopy to give **4** (30.1 mM, 421 μmol, 47%) as its chloride salt. ^{1}H NMR (500 MHz, D_2O, with acetone as the reference) δ: 7.85 (1H, d, J = 9.2 Hz, H-6), 6.97 (1H, t, J = 9.2 Hz, H-5), 4.43−4.46 (1H, m, CH), 4.36−4.43 (1H, m, H-2), 4.23−4.29 (1H, m, H-2), 3.97 (3H, s, OMe), 3.08−3.22 (2H, m, H-3), 1.51 (3H, d, J = 6.7 Hz, Me). HR−MS (FAB): calcd for $(C_{12}H_{16}N_3O_4)^+$, 266.1141; found, 266.1138.

Expression of Transporters in Human Embryonic Kidney (HEK)293 Cells. The cDNA coding for the rat ASCT2 was kindly provided by S. Bröer and was subcloned into the *Eco*RI site of the pBK-CMV vector (Stratagene) for mammalian expression. The coding sequences of rat SNAT1 and

SNAT2 were kindly provided by H. Varoqui and were subcloned into pBK-CMV (Stratagene). The ASCT2, SNAT1, and SNAT2 cDNA constructs were used for transient transfection of subconfluent HEK293 cells (ATCC number CGL 1573) using the calcium phosphate-mediated transfection method as described (*12*) or the commercially available Fugene reagent (Roche) according to the protocol provided by the supplier. Electrophysiological recordings were performed between days 1 and 3 post-transfection.

Whole-Cell Current Recording. Transporter currents were measured at room temperature in the whole-cell current-recording configuration (*24*) as described earlier (*12*). For experiments with ASCT2, the intracellular solution contained 140 mM NaSCN, 10 mM alanine, 1 mM $MgCl_2$, 10 mM ethylene glycol-bis(2-aminoethylether)-*N*,*N*,*N*′,*N*′-tetraacetic acid (EGTA), and 10 mM 4-(2-hydroxyethyl)piperazine-1-ethanesulfonic acid (HEPES) (pH 7.3) for experiments with ASCT2 (exchange conditions). We used NaSCN because ASCT2 is a neutral amino acid exchanger and does not catalyze steady-state transport current. However, under exchange conditions, a permanent anion current, carried by SCN^-, is catalyzed by this transporter (*25*). For SNAT1 and SNAT2, a solution containing 140 mM KCl, 2 mM $MgCl_2$, 10 mM EGTA, and 10 mM HEPES (pH 7.3) was used in the recording pipette. The extracellular solution contained 140 mM NaCl, 2 mM $MgCl_2$, 2 mM $CaCl_2$, and 10−30 mM HEPES (pH 7.3 for ASCT2 and pH 8.0 for SNAT1 and SNAT2). The typical resistance of the recording electrode was 2−3 MΩ; the series resistance was 4−6 MΩ. Because of the small whole-cell currents (less than 100 pA), series resistance compensation was not necessary. The currents were amplified with an Adams and List EPC-7 amplifier, low-pass-filtered at 1−10 kHz (Krohn−Hite 3322), and digitized with a digitizer board (Axon, Digidata 1200) at a sampling rate of 10−50 kHz, which was controlled by software (Axon PClamp).

Laser-Pulse Photolysis and Rapid Solution Exchange. Laser-pulse photolysis experiments were performed as described previously (*12*, *26*). Briefly, the cells were equilibrated with neutral amino acids or MNI-alanine using a fast solution exchange device. MNI-alanine was typically applied to the cells 2−3 s before photolysis to ensure full equilibration of the cells with the caged compound. All compounds were dissolved in extracellular solution. MNI-alanine was stored at −80 °C as a 30 mM aqueous stock solution, which was diluted with extracellular buffer to the working concentration (maximally 3 mM) prior to the experiment. The velocity of the solution emerging from the porthole of the device was 5 cm/s, and the time resolution was 20−30 ms (10−90% rise time with whole cells). Photolysis was initiated with a light flash generated by an excimer laser (Lambda Physik, MINEX), pumped by a homemade dye laser using *p*-terphenyl as the laser dye (5 mM solution in dioxan, $\lambda_{em} = 340$ nm, $t_{1/2} = 15$ ns), as described in ref *12*. The laser light was delivered to the cell with an optical fiber (350 μm diameter), and its energy was adjusted with neutral density filters (Andover Corporation). Typical laser energies, measured at the emitting end of the optical fiber using an energy meter (Gentec), were in the range of 50−400 mJ/cm^2. A standard alanine concentration of 1 mM was applied to the cell by rapid solution exchange before and after laser-pulse photolysis to estimate the concentration of photolytically released alanine and to test the cell for damage by the laser pulse, as described previously (*18*, *21*, *26*). Briefly, photolysis-induced steady-state currents (after decay of the transient components) at subsaturating alanine concentrations were compared with the steady-state current evoked by 1 mM free alanine and calibrated using an appropriate alanine dose−response curve for each transporter, as illustrated for ASTC2 in parts A−C of Figure 4. Alanine dose−response curves were obtained by applying alanine at various concentrations to the transporter-expressing cells with a rapid solution exchange device and measuring the alanine-evoked steady-state current at each concentration. The dashed line in Figure 4 represents the current used for scaling the dose−response curve to the 1 mM free alanine response, and the dotted line represents the current used to determine the concentration of the photolytically liberated alanine. We estimate the error for this determination of the alanine concentration as ±20%.

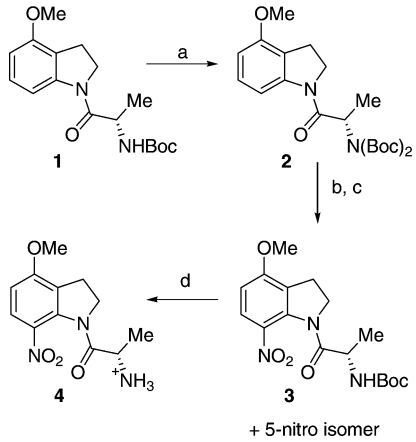

FIGURE 1: Reaction scheme for the synthesis of MNI-alanine: (a) $(Boc)_2O-Et_3N-DMAP-CH_2Cl_2$, (b) Claycop−$Ac_2O-CCl_4$, (c) 1 M TFA−$CH_2Cl_2$, and (d) neat TFA.

Determination of the Quantum Yield of Photolysis. To estimate the quantum yield, we used MNI-glutamate with a known photolysis quantum yield of 0.085 (*29*) as an actinometer. Separate solutions of MNI-alanine and MNI-glutamate (each ∼1 mM in extracellular buffer at pH 7.3) were placed in 1.5 × 3 mm cuvettes of 1.5 mm path length, irradiated with consecutive flashes of laser light at 351 nm at an energy density of 0.27 mJ/mm^2. Product formation after each laser flash was determined by measuring the absorbance at 404 nm (Thermoelectron Genesys 6 spectrophotometer) until complete photolysis was achieved. The extent of product formation was extrapolated to the first laser flash, and the values obtained were almost identical for both compounds. At the energy density used in these experiments, 6% of MNI-alanine was photolyzed after the first laser flash. When this value was extrapolated to the energy density of 1.2 mJ/mm^2 and assuming the absence of nonlinear effects, a single-flash conversion efficiency of 26% can be estimated for the conditions used in the cell photolysis experiments. This value compares well with the 27% conversion efficiency determined from the current calibration experiments.

RESULTS

*Synthesis and Photochemical Properties of MNI-Alanine **4**.* The synthetic route, outlined in Figure 1, followed

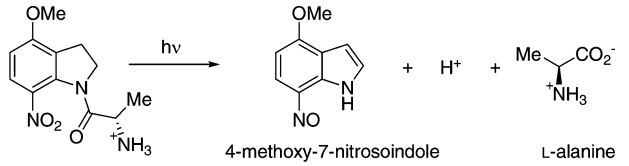

FIGURE 2: Photolysis reaction of MNI-alanine.

procedures previously established for optimal preparation of MNI-caged amino acids. Thus, the conjugate **1** was protected as its di-Boc derivative **2**, which minimizes unwanted nitration reactions at the amino nitrogen (*27*). Nitration of **2** (*28*) and treatment with dilute TFA to remove the second Boc group (*27*) gave predominantly the 7-nitro isomer **3** after silica gel chromatography. This material, without full purification, was treated with neat TFA to remove the last Boc group. Preparative reverse-phase HPLC then gave pure **4**, free of any contamination by the 5-nitro isomer. Unlike previous syntheses of MNI-protected amino acids, the present compound could be freed of buffer salts after the preparative HPLC procedure by careful basification that allowed extraction of the uncharged compound into the organic solvent. Evaporation of this solvent and adjustment of an aqueous suspension to pH 7 gave **4** as its chloride salt that was readily water-soluble.

MNI-alanine showed a broad peak in its UV−vis spectrum (λ_{max} = 327 nm) that was red-shifted by ~5 nm from that of the reference *N*-acetyl compound previously described (*29*). Nevertheless, we used the extinction coefficient of 4800 M^{-1} cm^{-1} determined for the reference compound to quantify aqueous solutions. Photolysis followed the expected course (data not shown) as indicated by the appearance of a new absorption with λ_{max} = 404 nm, consistent with the previously identified 4-methoxy-7-nitrosoindole byproduct. The quantum yield for photolysis was determined as 0.084, essentially identical to the value previously determined for MNI-glutamate (*29*). The reaction spectrum showed three clean isosbestic points at wavelengths of 262, 308, and 363 nm, as expected from previously published results of a MNI-acetate model compound (*29*). The photolysis reaction is shown in Figure 2. We did not directly determine the rate of product release upon laser flash irradiation of MNI-alanine, but this rate is expected to be similar to that previously determined for a nitroindoline-caged acetate model compound in a detailed study of nitroindoline photolysis, where the time constant for product release was found to be 200 ns (*22*). As shown below, the fastest reaction observed in the transporters studied here occurs with a time constant of about 100 μs, which is 500-fold slower than the time constant of alanine release expected from the previous study. It is highly unlikely that a change in the leaving group from acetate to alanine could result in such a large change in the photolysis rate, given the otherwise identical photochemical behavior of the two compounds. Therefore, we assume that photolytic alanine release is not rate-limiting for the transporter processes studied here.

Characterization of Biological Properties of MNI-Alanine with Respect to Amino Acid Transporters. We first tested whether MNI-alanine is a transported substrate or inhibitor of ASCT2, SNAT1, and SNAT2. When MNI-alanine was applied to an ASCT2-expressing cell at a concentration of 3 mM, no current response was observed (Figure 3B, n = 4).

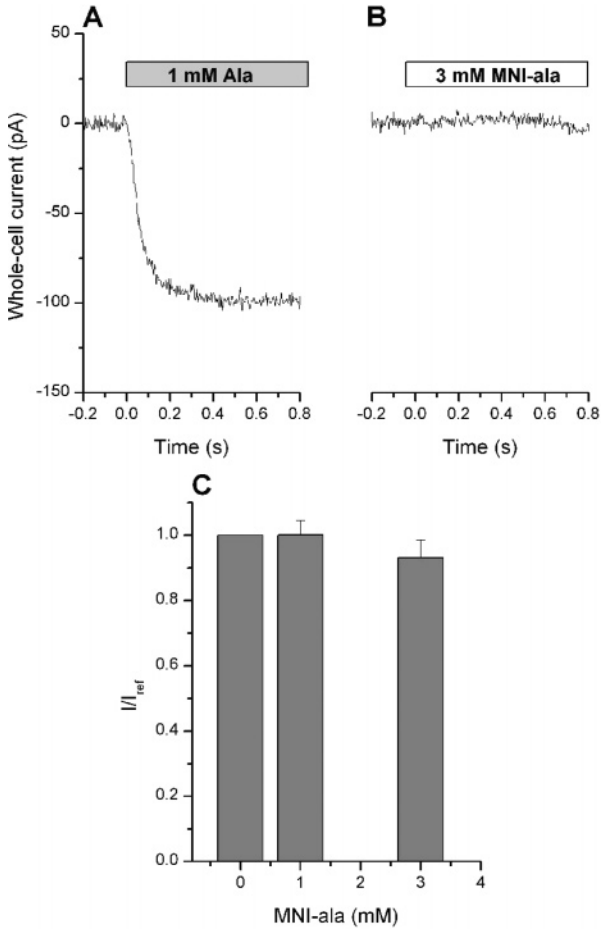

FIGURE 3: MNI-alanine is biologically inactive with respect to ASCT2. (A) Typical anion current induced by the application of 1 mM alanine by rapid solution exchange, as indicated by the gray bar. (B) Application of 3 mM MNI-alanine to the same cell as in A did not result in any measurable current. (C) Co-application of MNI-alanine at concentrations of up to 3 mM with 1 mM free alanine to ASCT2 did not reduce the anion current. The transmembrane potential was 0 mV. I_{ref} is the current evoked by rapid solution exchange with 1 mM alanine in the absence of MNI-alanine.

Table 1: Steady-State Kinetic Parameters of the Current Activation by Alanine of the Amino Acid Transporters Studied (0 mV Transmembrane Potential)

	K_m (alanine) (μM)	I_{max} (pA)
ASCT2	415 ± 30	−140 ± 31 (n = 10)
SNAT1	520 ± 80	−75 ± 15 (n = 7)
SNAT2	200 ± 17	−107 ± 27 (n = 11)

In contrast, the application of 1 mM free alanine elicited an inwardly directed anion current of −140 ± 31 pA (Figure 3A, n = 10) in the same cells. This concentration of alanine saturates about 75% of the ASCT2 substrate-binding sites (the apparent K_m values of the transporters for alanine determined in this work are listed in Table 1). Similarly, the application of 2 mM MNI-alanine to SNAT1-expressing cells elicited no detectable current response (n = 3), whereas the application of 4 mM alanine (a saturating concentration) induced −75 ± 15 pA (n = 7, data not shown). Similar data were obtained for SNAT2 (not shown). Together, these data indicate that MNI-alanine is not transported by these three amino acid transporters at the concentrations tested. Furthermore, the results suggest that the background concentration of free alanine in the caged compound is very low, as

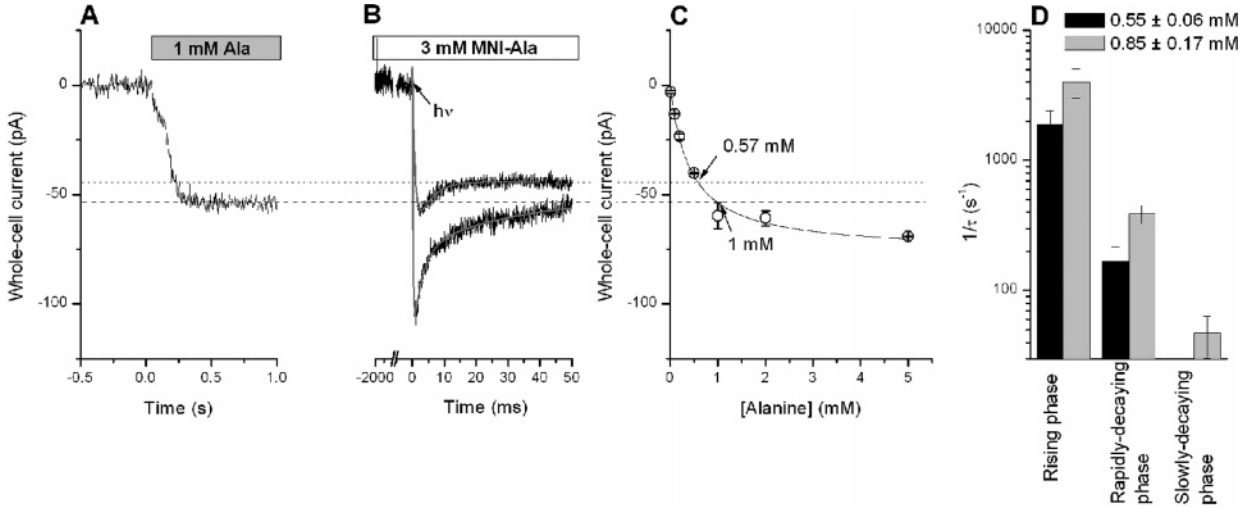

FIGURE 4: Photolysis of MNI-alanine generates anion currents in ASCT2 expressing HEK293 cells. (A) Steady-state current induced by the application of 1 mM alanine by rapid solution exchange, as indicated by the gray bar. The intracellular solution contained 140 mM SCN^-. (B) Typical pre-steady-state anion current recorded from ASCT2 in the same cell as in A upon photolytic release from 3 mM MNI-alanine at time 0, as indicated by the arrow. Pre-equilibration with MNI-alanine for 2 s prior to the laser flash is indicated by the white bar. The transmembrane potential was 0 mV. The two curves represent traces at two different concentrations of alanine (0.55, upper trace; 0.85 mM, lower trace) obtained by varying the laser intensity. (C) Alanine dose−response curve of ASCT2 anion current used for the calibration procedure to estimate the concentration of amino acid released by photolysis. (D) Statistical analysis of the relaxation rate constants obtained at two alanine concentrations ($V = 0$ mV). The slowly decaying phase was absent at the lower alanine concentration.

expected from previous data on the stability of nitroindoline-caged compounds (*30*).

Next, we determined whether the MNI-caged compound inhibits transporter function. To test this, we co-applied MNI-alanine and free alanine to the transporters and compared the current amplitude with that generated in the same cell by the application of alanine in the absence of the caged compound. Figure 3C shows that co-application of up to 3 mM MNI-alanine (the maximum concentration used in the photolysis experiments) with 1 mM free alanine to cells expressing ASTC2 did not result in a significant reduction of the alanine-induced anion current. Similarly, no inhibition was observed with SNAT1 and SNAT2, where co-application of 2 mM MNI-alanine together with 0.5 mM free alanine (0.2 mM for SNAT2) elicited 1.05 ± 0.38 times ($n = 4$; SNAT1) and 0.99 ± 0.14 times ($n = 4$; SNAT2) the current response to the application of the same concentration of free alanine alone. For these inhibition experiments, the concentrations of free alanine were chosen to saturate approximately half of the binding sites of the respective transporter population with alanine (see Table 1 for K_m values of SNAT1 and SNAT2 for alanine), to maximize potential inhibitory effects of MNI-alanine. The maximum MNI-alanine concentration tested in photolysis experiments with SNAT1 and SNAT2 was 2 mM. Together, these data suggest that MNI-alanine is biologically inert toward the transporters ASCT2, SNAT1, and SNAT2 and, thus, can be used in laser photolysis experiments to determine the kinetics of neutral amino acid transport by these systems.

ASCT2 Pre-steady-State Kinetics. The time dependencies of the current responses of an ASCT2-expressing cell to the application of alanine by rapid solution exchange (Figure 4A) or photolysis of MNI-alanine (Figure 4B) are distinctly different from each other. The anion current induced by 1 mM alanine applied by rapid solution exchange rises to a maximum without showing any overshoot current component. The rise of this current is limited by the time resolution of the solution exchange system (20−50 ms) and thus does not contain any kinetic information on the transporter. In contrast, photolytic release of alanine (850 μM, estimated from the photolysis-induced steady-state current relative to the steady-state current generated by 1 mM alanine and the K_m for alanine, Table 1, as shown in Figure 4C) from the caged precursor (3 mM) generates a transient current component that precedes the steady-state anion current. This transient current component shows a double-exponential decay, with time constants of 3.1 ± 0.2 and 35 ± 7 ms ($n = 4$). The rapidly decaying component has a relative amplitude twice that of the slowly decaying phase. The rise of the anion current is extremely rapid and occurs with a time constant of 0.2 ± 0.1 ms ($n = 4$). The combined results demonstrate that activation of the anion current by alanine in ASCT2 is associated with rapid processes, occurring on a sub-millisecond to millisecond time scale. The pre-steady-state kinetics of the ASCT2 anion current were dependent upon the alanine concentration (parts B and D of Figure 4). The amplitude of the transient phase of the current decreased when the alanine concentration was lowered to 550 μM. The relaxation rate constants for the current rise and the rapidly decaying phase also decreased at lower alanine concentrations (Figure 4D), as expected for an alanine-dependent transport process. The slowly decaying phase was absent at 550 μM alanine (Figure 4B).

Photolysis of caged compounds by a 15 ns laser pulse can lead to artifacts in current recordings, owing to the high peak power of the laser radiation. To control for possible artifacts and to check the specificity of the photolysis-induced current signal, we performed control experiments in the absence of extracellular Na^+. Because ASCT2 is a Na^+-coupled amino acid exchanger (*7*, *9*, *31*), it is expected that the absence of Na^+ will lead to a reduction or elimination of the alanine-induced anion current. In agreement with this expectation, photolysis of MNI-alanine did not induce any currents (Figure 5B, control in the presence of Na^+ is shown in Figure

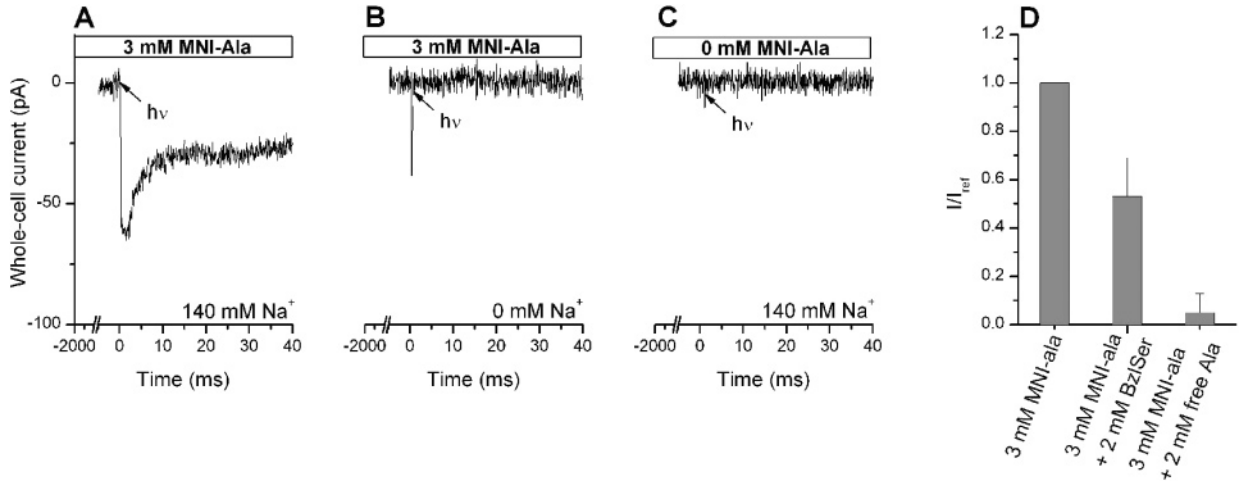

FIGURE 5: ASCT2 anion currents induced by photolysis of MNI-alanine are specifically carried by the transporter. (A) Pre-steady-state anion current recorded from ASCT2 after photolytic release from 3 mM MNI-alanine in the presence of 140 mM extracellular Na^+. (B) Same experiment as in A but in the absence of extracellular Na^+. (C) Current recording from the same cell in the absence of caged alanine. The laser was flashed at time $t = 0$ s. (D) Steady-state anion currents generated by photolytic release of alanine from 3 mM MNI-alanine are inhibited by the co-application of the competitive ASCT2 inhibitor BzlSer (2 mM) or 2 mM free alanine. In the experiment with free 2 mM free alanine, only the photolysis-induced current is shown, which is in addition to the steady-state current elicited by the free alanine. The transmembrane potential was 0 mV. I_{ref} is the current evoked by photolysis of 3 mM MNI-alanine in the absence of the inhibitor or alanine.

5A) when extracellular Na^+ was replaced with *N*-methyl-glucamine$^+$ (NMG^+), a cation that does not interact with the ASCT2 Na^+-binding site(s) (*25*). Evidently, alanine cannot mediate an anion current in ASCT2 without Na^+ being present, in line with observations previously made for the homologous glutamate transporters of the SLC1 family (*13*, *14*). Further control experiments are shown in parts C and D of Figure 5. A laser flash applied to an ASCT2-expressing cell in the absence of MNI-alanine did not elicit any current response, eliminating the possibility of nonspecific currents caused by the laser light. When photolysis was performed in the presence of 2 mM benzylserine (BzlSer), a competitive inhibitor of ASCT2 (*25*), the anion current was reduced to 53 ± 16% ($n = 5$) of that in the absence of the inhibitor. Photolysis was also performed in the presence of 2 mM free alanine, a concentration that should fully preactivate the ASCT2 anion current. Under these conditions, photolysis of MNI-alanine induced little further transient and steady-state anion current above that already activated by the free alanine (Figure 5D). This result is expected because 85% of the binding sites of ASCT2 should already be occupied by free alanine before photolyis was initiated. Together, these results indicate that the steady-state and transient anion currents shown in Figure 4 were specifically generated by ASCT2.

SNAT1 Pre-steady-State Kinetics. Photolytic release from 2 mM MNI-alanine induced transport currents in SNAT1-expressing HEK293 cells (Figure 6B). Under zero-*trans* conditions (quasi-zero concentrations of the substrates on the intracellular, *trans* side of the membrane), these currents were inwardly directed. An inward current is expected for electrogenic operation of SNAT1 because it co-transports the neutral amino acid substrate, presumably with one Na^+ ion, into the cell (*4*, *16*). Before the steady state was reached, a transient component of the current was observed, decaying with a time constant of 1.3 ± 0.2 ms ($n = 3$). Thus, it appears that a rapid, electrogenic partial reaction of the transporter precedes steady-state turnover. The rise of the electrogenic transport current occurred within the time resolution limit

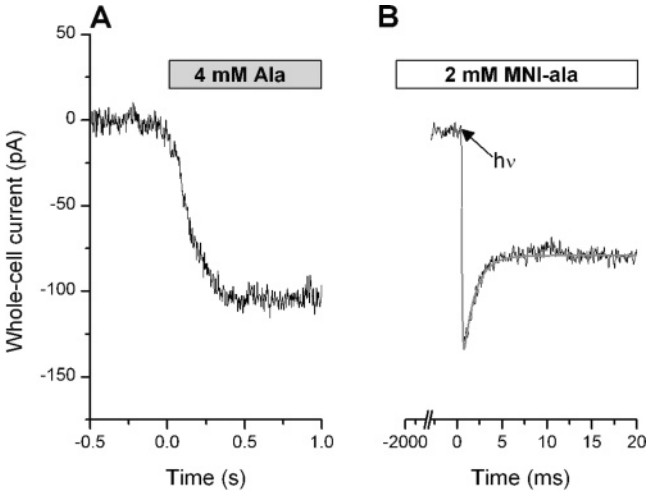

FIGURE 6: Photolysis of MNI-alanine generates transport currents in SNAT1-expressing HEK293 cells. (A) Steady-state current induced by the application of 4 mM alanine by rapid solution exchange, as indicated by the gray bar. (B) Typical pre-steady-state current recorded from SNAT1 in the same cell as in A upon photolytic release from 2 mM MNI-alanine at time 0, as indicated by the arrow. Pre-equilibration with MNI-alanine for 2 s prior to photolysis is indicated by the white bar. The transmembrane potential was 0 mV.

of the recording system imposed by the 3 kHz filtering frequency (i.e., 100 μs range) after photorelease of alanine. It remains to be determined whether the onset of the transient current is really instantaneous or whether it is preceded by a fast electroneutral reaction that delays the electrogenic current component. Better time resolution of the recording system would be necessary to investigate this point.

The concentration of alanine released from 2 mM of the caged precursor was estimated as 600 μM by a comparison with data from the application of 4 mM free alanine to the same cell (Figure 6A) and the dose−response curve for alanine activation of the SNAT1 current (the K_m for alanine activation of the steady-state transport current was determined to be 520 ± 80 μM, Table 1). Thus, it is feasible to

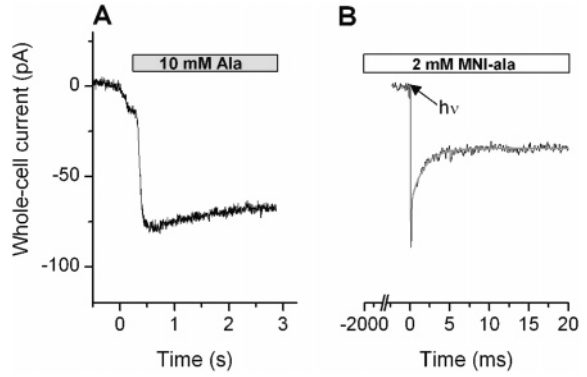

FIGURE 7: Photolysis of MNI-alanine generates transport currents in SNAT2-expressing HEK293 cells. (A) Steady-state current induced by the application of 10 mM alanine by rapid solution exchange, as indicated by the gray bar. (B) Typical pre-steady-state current recorded from SNAT2 in the same cell as in A upon photolytic release from 2 mM MNI-alanine at time 0, as indicated by the arrow. Pre-equilibration with MNI-alanine for 2 s prior to photolysis is indicated by the white bar. The transmembrane potential was 0 mV.

photorelease concentrations of alanine from 2 mM MNI-alanine that at least half-saturate the SNAT1 alanine-binding site.

SNAT2 Pre-steady-State Kinetics. Photolytic release of alanine was also used to determine the pre-steady-state kinetics of transport currents carried by the system A isoform SNAT2. As shown in Figure 7A, flow application of alanine induced large inwardly directed currents in SNAT2-expressing HEK293 cells. Photolytic release from 2 mM MNI-alanine at the same cell resulted in an inward current of similar amplitude but also revealed a rapidly decaying transient phase (Figure 7B). The time constant of the decay of this transient current was 1.6 ± 0.1 ms ($n = 3$). As with SNAT1, the alanine-induced current in SNAT2 was activated within the time resolution of the recording after photolytic alanine release. Hence, at least one rapid, voltage-dependent reaction precedes steady-state alanine transport.

DISCUSSION

In this work, we have synthesized a new caged alanine derivative protected with the photolabile 4-methoxy-7-nitroindolinyl caging group and characterized its biological properties. MNI-alanine was synthesized according to established procedures from readily available starting materials. The compound is stable in aqueous solution and photolyzes efficiently to produce free alanine. MNI-alanine was found to be biologically inert with respect to three neutral amino acid transporters, namely, ASCT2, SNAT1, and SNAT2.

The new caged alanine derivative was used to generate alanine concentration jumps, thereby achieving rapid activation of transport-associated currents in ASCT2 expressed in HEK293 cells. Photolysis of a 3 mM MNI-alanine solution liberates concentrations of free alanine up to about 800 μM (a concentration about double the K_m value of ASCT2 for alanine of 415 μM, Table 1), as tested by a comparison of photolysis-induced currents with those induced by the application of a saturating concentration of alanine to ASCT2 with a rapid solution exchange method. This result, together with our data determining photolysis efficiency by absorption spectroscopy, shows that MNI-alanine photolyzes efficiently under the conditions used, liberating nearly 27% of the protected alanine upon photolysis with a single laser flash. Activation of ASCT2 anion currents occurs on a submillisecond time scale, and the rapid photolytic release of alanine revealed three phases of the current that were not observed in previous solution exchange experiments on transfected HEK293 cells (*25*) or ASCT2-expressing *Xenopus* oocytes (*7*). These phases represent rapid, substrate-induced reactions of the transporter protein. Although the exact assignment of these phases to specific partial reactions in the ASCT2 transport mechanism will require further experimentation, several preliminary conclusions can be drawn from these results. (1) The fastest phase observed in the pre-steady-state experiments is the rising phase of the anion current, which may be rate-limited by alanine binding. If this is the case, we can estimate a lower limit of the bimolecular binding rate constant of the transporter for alanine as 7×10^6 M^{-1} s^{-1}. This binding rate is comparable to the binding rates of glutamate to the glutamate transporters of the SLC1 family [$1-2 \times 10^7$ M^{-1} s^{-1} (*12*)] that are related to ASCT2. (2) Two rapid processes induced by alanine binding occur on a 3−35 ms time scale. Because Na^+ and alanine were present at high concentrations on the intracellular side of the membrane, it is unlikely that the reactions generating these two phases of the anion current arise from dissociation of the substrate or Na^+ to the cytosol. Instead, these phases might be caused either by Na^+ binding to the extracellular side of the transporter and/or the translocation reaction. At present, we cannot differentiate between these two possibilities. (3) The slowest process observed has a time constant of 35 ms, suggesting that ASCT2 operates relatively slowly. If this process was rate-limiting for amino acid exchange, it would mean that no more than about 30 alanine molecules per second could be exchanged across the membrane by ASCT2 at steady state and 0 mV transmembrane potential. (4) No anion current signal was induced by photolytic application of alanine in the absence of extracellular Na^+, which suggests either that alanine cannot bind to ASCT2 in the absence of Na^+ or that it can bind without activating an anion current. It has been shown previously that ASCT2 requires Na^+ to enable amino acid transport (*7*). Our results demonstrate that the presence of extracellular Na^+ is also required to generate an anion current. These results mirror findings obtained with the glutamate transporters of the SLC1 family, showing that the substrate-induced anion conductance is gated by the binding of Na^+ to the transporter (*14*).

The generation of alanine concentration jumps by photolysis of the new caged alanine derivative enabled us to determine the pre-steady-state kinetics of two members of the SLC38 family of transporters, SNAT1 and SNAT2. In both transporter isoforms, photorelease of alanine generated rapidly decaying transient currents that relaxed to a steady-state current within about 5 ms. Interestingly, the time constants of the decay of this transient current, as well as the peak current/steady-state current ratio, were similar for SNAT1 and SNAT2, indicating that these two transporter subtypes do not significantly differ from each other in the kinetics of alanine transport. The results obtained here for SNAT1 can be compared with a previous study, in which pre-steady-state currents were generated by stepping the transmembrane potential (*16*). Those transient currents

relaxed with a time constant of 4−5 ms, significantly slower than the time constant of 1.3 ms of the alanine-induced transient current observed here. This indicates that the pre-steady-state processes observed in the voltage jump and concentration jump experiments are not identical. In fact, the transient current induced by a voltage jump was proposed to be caused by electrogenic association of Na^+ with the alanine-free transporter form, occurring with an apparent valence of 0.7 (*16*). Because the proposed stoichiometry of Na^+−alanine co-transport is 1:1, a total of 1 positive charge is moved into the cell for each transported alanine molecule. If this stoichiometry is correct, another 30% of the total SNAT1 charge movement would be unaccounted for by voltage-dependent Na^+ binding. Thus, an additional electrogenic reaction would be required in the transport cycle. It is likely that the fast electrogenic process observed here contributes to the remaining 30% of the total charge movement. This process is unlikely to be rate-limiting for the steady-state turnover of SNAT1, because it is faster than the Na^+-binding reaction observed by Mackenzie and colleagues (*16*).

The "instantaneous" generation of the inward current after the alanine concentration jump in SNAT1 and SNAT2 indicates that the electrogenic reaction associated with this transient current is either the first step in a sequence of reactions induced by alanine or that an extremely rapid electroneutral reaction, faster than the time resolution of our method, precedes this electrogenic process. Because alanine is a zwitterion at neutral pH and, therefore, has no net charge, it is likely that the alanine-binding process itself is electroneutral, even if binding occurs within the membrane electric field. If this assumption is correct, then alanine binding to SNAT1 and SNAT2 must be rapid, with a bimolecular rate constant $> 2 \times 10^7\ M^{-1}\ s^{-1}$.

In conclusion, we have shown that a new caged alanine derivative, MNI-alanine, synthesized here has favorable photochemical and biological properties. Concentration jumps generated by photolytic release of alanine from this caged precursor allowed us to observe alanine-induced pre-steady-state currents of three different neutral amino acid transporters belonging to two different SLC families. These pre-steady-state currents contain significant, new information on the molecular mechanism of electrogenic and electroneutral transport of small, neutral amino acids. This caged compound will also be useful for the functional investigation of the amino acid transporters in their native brain environment. Because neutral amino acid transporters are involved in the glutamate−glutamine cycle (*1*, *32*) and, thus, in the recycling of synaptically released glutamate, the detailed investigation of their molecular function at the synapse is important.

ACKNOWLEDGMENT

We thank Dr. S. Bröer for making available cDNA encoding ASCT2 and Dr. H. Varoqui for cDNA encoding SNAT1/2. We are grateful to Dr. V. R. N. Munasinghe for recording ^1H NMR spectra and to the MRC Biomedical NMR Centre for access to facilities.

REFERENCES

1. Bode, B. P. (2001) Recent molecular advances in mammalian glutamine transport, *J. Nutr. 131*, 2475S−2485S.
2. Mackenzie, B., and Erickson, J. (2004) Sodium-coupled neutral amino acid (system N/A) transporters of the SLC38 gene family, *Pfluegers Arch. 447*, 784−795.
3. Varoqui, H., Zhu, H. M., Yao, D., Ming, H., and Erickson, J. D. (2000) Cloning and functional identification of a neuronal glutamine transporter, *J. Biol. Chem. 275*, 4049−4054.
4. Sugawara, M., Nakanishi, T., Fei, Y.-J., Huang, W., Ganapathy, M. E., Leibach, F. H., and Ganapathy, V. (2000) Cloning of an amino acid transporter with functional characteristics and tissue expression pattern identical to that of system A, *J. Biol. Chem. 275*, 16473−16477.
5. Chaudhry, F. A., Krizaj, D., Larsson, P., Reimer, R. J., Wreden, C., Storm-Mathisen, J., Copenhagen, D., Kavanaugh, M., and Edwards, R. H. (2001) Coupled and uncoupled proton movement by amino acid transport system N, *EMBO J. 20*, 7041−7051.
6. Nakanishi, T., Kekuda, R., Fei, Y.-J., Hatanaka, T., Sugawara, M., Martindale, R. G., Leibach, F. H., Prasad, P. D., and Ganapathy, V. (2001) Cloning and functional characterization of a new subtype of the amino acid transport system N, *Am. J. Physiol. 281*, C1757−C1768.
7. Bröer, A., Wagner, C., Lang, F., and Bröer, S. (2000) Neutral amino acid transporter ASCT2 displays substrate-induced Na^+ exchange and a substrate-gated anion conductance, *Biochem. J. 346*, 705−710.
8. Utsunomiya-Tate, N., Endou, H., and Kanai, Y. (1996) Cloning and functional characterization of a system ASC-like Na^+-dependent neutral amino acid transporter, *J. Biol. Chem. 271*, 14883−14890.
9. Zerangue, N., and Kavanaugh, M. P. (1996) ASCT-1 is a neutral amino acid exchanger with chloride channel activity, *J. Biol. Chem. 271*, 27991−27994.
10. Sokolov, V. S., Apell, H. J., Corrie, J. E. T., and Trentham, D. R. (1998) Fast transient currents in Na,K-ATPase induced by ATP concentration jumps from the P^3-[1-(3′,5′-dimethoxyphenyl)-2-phenyl-2-oxo]ethyl ester of ATP, *Biophys. J. 74*, 2285−2298.
11. Stengelin, M., Fendler, K., and Bamberg, E. (1993) Kinetics of transient pump currents generated by the (H,K)-ATPase after an ATP concentration jump, *J. Membr. Biol. 132*, 211−227.
12. Grewer, C., Watzke, N., Wiessner, M., and Rauen, T. (2000) Glutamate translocation of the neuronal glutamate transporter EAAC1 occurs within milliseconds, *Proc. Natl. Acad. Sci. U.S.A. 97*, 9706−9711.
13. Wadiche, J. I., Arriza, J. L., Amara, S. G., and Kavanaugh, M. P. (1995) Kinetics of a human glutamate transporter, *Neuron 14*, 1019−1027.
14. Watzke, N., Bamberg, E., and Grewer, C. (2001) Early intermediates in the transport cycle of the neuronal excitatory amino acid carrier EAAC1, *J. Gen. Physiol. 117*, 547−562.
15. Loo, D. D. F., Hazama, A., Supplisson, S., Turk, E., and Wright, E. M. (1993) Relaxation kinetics of the Na^+/glucose cotransporter, *Proc. Natl. Acad. Sci. U.S.A. 90*, 5767−5771.
16. Mackenzie, B., Schafer, M. K.-H., Erickson, J. D., Hediger, M. A., Weihe, E., and Varoqui, H. (2003) Functional properties and cellular distribution of the system A glutamine transporter SNAT1 support specialized roles in central neurons, *J. Biol. Chem. 278*, 23720−23730.
17. Wadiche, J. I., and Kavanaugh, M. P. (1998) Macroscopic and microscopic properties of a cloned glutamate transporter/chloride channel, *J. Neurosci. 18*, 7650−7661.
18. Bicho, A., and Grewer, C. (2005) Rapid substrate-induced charge movements of the GABA transporter GAT1, *Biophys. J. 89*, 211−231.
19. Goeldner, M., and Givens, R. S., Eds. (2005) *Dynamic Studies in Biology*, Wiley-VCH, Weinheim, Germany.
20. Canepari, M., Nelson, L., Papageorgiou, G., Corrie, J. E. T., and Ogden, D. (2001) Photochemical and pharmacological evaluation of 7-nitroindolinyl-and 4-methoxy-7-nitroindolinyl-amino acids as novel, fast caged neurotransmitters, *J. Neurosci. Methods 112*, 29−42.
21. Maier, W., Corrie, J. E. T., Papageorgiou, G., Laube, B., and Grewer, C. (2005) Comparative analysis of inhibitory effects of caged ligands for the NMDA receptor, *J. Neurosci. Methods 142*, 1−9.
22. Morrison, J., Wan, P., Corrie, J. E. T., and Papageorgiou, G. (2002) Mechanisms of photorelease of carboxylic acids from 1-acyl-7-nitroindolines in solutions of varying water content, *Photochem. Photobiol. Sci. 1*, 960−969.
23. Gangjee, A., Vasudevan, A., and Queener, S. F. (1997) Synthesis and biological evaluation of nonclassical 2,4-diamino-5-meth-

ylpyrido[2,3-*d*]pyrimidines with novel side chain substituents as potential inhibitors of dihydrofolate reductases, *J. Med. Chem. 40*, 479−485.
24. Hamill, O. P., Marty, A., Neher, E., Sakmann, B., and Sigworth, F. J. (1981) Improved patch-clamp techniques for high-resolution current recording from cells and cell-free membrane patches, *Pfluegers Arch. 391*, 85−100.
25. Grewer, C., and Grabsch, E. (2004) New inhibitors for the neutral amino acid transporter ASCT2 reveal its Na^+-dependent anion leak, *J. Physiol. 557*, 747−759.
26. Grewer, C., Jaeger, J., Carpenter, B. K., and Hess, G. P. (2000) A new photolabile precursor of glycine with improved properties: A tool for chemical kinetic investigations of the glycine receptor, *Biochemistry 39*, 2063−2070.
27. Papageorgiou, G., Ogden, D., and Corrie, J. E. T. (2004) An antenna-sensitized nitroindoline precursor to enable photorelease of L-glutamate in high concentrations, *J. Org. Chem. 69*, 7228−7233.
28. Papageorgiou, G., and Corrie, J. E. T. (2002) Regioselective nitration of 1-acyl-4-methoxyindolines leads to efficient synthesis of a photolabile L-glutamate precursor, *Synth. Commun. 32*, 1571−1577.
29. Papageorgiou, G., and Corrie, J. E. T. (2000) Effects of aromatic substitution on the photocleavage of 1-acyl-7-nitroindolines, *Tetrahedron 56*, 8197−8205.
30. Papageorgiou, G., Ogden, D. C., Barth, A., and Corrie, J. E. T. (1999) Photorelease of carboxylic acids from 1-acyl-7-nitroindolines in aqueous solution: Rapid and efficient photorelease of L-glutamate, *J. Am. Chem. Soc. 121*, 6503−6504.
31. Bröer, A., Brookes, N., Ganapathy, V., Dimmer, K. S., Wagner, C. A., Lang, F., and Bröer, S. (1999) The astroglial ASCT2 amino acid transporter as a mediator of glutamine efflux, *J. Neurochem. 73*, 2184−2194.
32. Chaudhry, F. A., Reimer, R. J., and Edwards, R. H. (2002) The glutamine commute: take the N line and transfer to the A, *J. Cell Biol. 157*, 349−355.

BI0620860